J Mol Model (2013) 19:2913–2924
DOI 10.1007/s00894-013-1822-z

ORIGINAL PAPER

Assessment of the photosensitization properties of cationic porphyrins in interaction with DNA nucleotide pairs

Gloria I. Cárdenas-Jirón · Luis Cortez

Received: 3 November 2012 / Accepted: 10 March 2013 / Published online: 14 April 2013

Abstract We present a theoretical assessment of the photosensitization properties of meso-mono(N-methylpyridyl) triphenylporphyrin (**1**, $MmPyP^+$), which interacts with DNA nucleotide pairs [adenine (A)-thymine (T); guanine (G)-cytosine (C)] via an external binding mode. The photosensitization properties of the arrangements **1A**, **1T**, **1G** and **1C** were investigated. A set of density functionals (B3LYP, PBE0, CAM-B3LYP, M06-2X, B97D) with the 6-31G(d) basis set was used to calculate the electronic absorption spectra in solution (water) following TD-DFT methodology. In all the arrangements, with the exception of **1C**, the functional PBE0 produced the lowest deviation of the Soret band (0.1–0.2 eV). Using this functional, we show that the porphyrin–nucleotide interaction is stabilized, as reflected by a larger HOMO–LUMO gap than free porphyrin. A more important effect of the interaction corresponds to the red-shift of the Soret band of $MmPyP^+$, which is in agreement with experimental results. This behavior could be explained by the higher symmetry found in arrangements with a lower dipole moment, and by the more symmetrical distribution of electronic density along the molecular orbitals, which provokes electronic transitions of lower energy. The structural model allowed us to show that $MmPyP^+$ improves the characteristics as a photosensitizer when it interacts with nucleotide pairs due to the longer wavelength required for the Soret band. Results obtained for porphyrins with larger monocationic substituents (**2**, MmAP+; **3**, MONPP+) do not lead to the same behavior. Although the structural model is insufficient to describe porphyrin photosensitization, it suggests that improvements in this property are produced by the inclusion of a cationic charge in the pyridyl ring and a smaller size of the substituent leading to a better communication in the porphyrin–nucleotide pair.

Keywords Porphyrin · DNA · Photosensitizer · Density functional theory · Sensor

Introduction

Porphyrin and its derivatives are studied widely due to their photophysical and electrochemical properties. There is growing interest in studying the interaction of specific drugs [1] with deoxyribonucleic acid (DNA) and porphyrins have attracted particular attention [2]. The ability of porphyrins to selectively cleave DNA, as a consequence of their photophysical properties, has led to these compounds being widely used as structural sensors of DNA [3, 4].

Cationic porphyrins bind strongly to DNA [5, 6], photodynamically modifying the target site of a DNA molecule, and thus becoming potential antitumor therapeutic agents [7]. The feature we wished to explore in this work was their ability as photosensitizers [8], which could be applied in photodynamic therapy (PDT) for the treatment of cancer and in virus inhibition [9–12].

According to the literature, water-soluble cationic porphyrins can bind DNA non-covalently in three ways: (1)

Electronic supplementary material The online version of this article (doi:10.1007/s00894-013-1822-z) contains supplementary material, which is available to authorized users.

G. I. Cárdenas-Jirón (✉) · L. Cortez
Laboratorio de Química Teórica, Facultad de Química y Biología, Universidad de Santiago de Chile (USACH), Casilla 40, Correo 33, Santiago, Chile
e-mail: gloria.cardenas@usach.cl

intercalation between base pairs, (2) outside binding toward the phosphate group without stacking, and (3) outside binding with stacking toward the grooves [3, 13–17]. It has been observed for porphyrins with similar sizes of cationic substituent that intercalation and outside binding depend strongly on the electronic structure [18].

Among the simple cationic porphyrins, the tetracationic water soluble 5,10,15,20-tetrakis(4-methyl-pyridyl)porphyrin (TMPyP) has been widely studied. Studies show a variety of activities, including high affinity with nucleic acids and preferential localization in tumor tissues [19], photodynamic inactivation of fungi [20], HCl gas sensing in composite with TiO_2 [21], photo-inactivation of Gram-negative bacteria [22], interaction with biological membranes [23], among others.

Despite good experimental evidence from UV–vis spectroscopy of the affinity of cationic porphyrins for DNA, the effect that DNA produces on porphyrin at the level of its molecular structure that results in changes in the UV–vis spectra with respect to porphyrin in its isolated form remains unclear.

Taking into account the computational cost of tetracationic porphyrins, we explored the study of a monocationic porphyrin: meso-mono(N-methylpyridyl) triphenylporphyrin (**1**, $MmPyP^+$) (Fig. 1). The aim of this work was to investigate from a quantum chemistry point of view why the photosensitization properties of monocationic porphyrins are modified by the existence of an interaction with DNA nucleotide pairs. For this purpose, we performed a theoretical study of the singlet excited state properties of **1** interacting with nucleotide pairs by outside binding [24]. We analyzed the characteristic bands of porphyrin in the UV–vis spectrum, Soret and Q, for each arrangement of porphyrin–DNA and evaluated the contribution of the fragments from a molecular orbital viewpoint. We also investigated the effect of the size of the monocationic substituent.

Computational aspects

We studied one monocationic porphyrin (**1**) (Fig. 1) and its interaction with a nucleotide pair (adenine-thymine, **AT**, guanine-cytosine, **GC**), giving the arrangements **1A**, **1T**, **1G** and **1C**, by outside binding following the structural model displayed in Fig. 1. In order to investigate the effect of monocationic substituent size on the photosensitization properties, we included in our study two monocationic porphyrins (**2**, **3**) (Fig. 1) and their respective arrangements (**2A**, **2T**, **2G**, **2C** and **3A**, **3T**, **3G**, **3C**). Optimized molecular geometries in the gas phase for all the supramolecular arrangements were obtained using a three layer ONIOM [25–27] model as published elsewhere [24] with the Gaussian03 package [28]. Note that the reason for using ONIOM was to reduce the computational cost because of the large size of the arrangements. The latter have ~160–180 atoms and ~1,500–1,700 basis functions. In the geometry optimization, for the region corresponding to the outside binding ($N^+CH_3\cdots PO_4^-$) we used density functional theory (DFT) with the functional and basis set B3LYP/6-31G(d) [29–31], the semiempirical PM3 method [32] for the base pair and the porphyrin, and molecular mechanics with the universal force field UFF [33] for the ribose units. PM3 has been shown to be enough to obtain a geometry that treats the hydrogen bonding between nitrogenous bases reasonably [24, 34, 35]. However, the energetic aspects require to be treated with a higher level theoretical method.

For comparison, isolated porphyrins were optimized under the same conditions as for the supramolecular arrangements, i.e., the cationic substituent with B3LYP/6-31G(d) and the triphenyl porphyrin with the semiempirical PM3 method. The nature of the stationary points was verified by analytical calculations of harmonic vibrational frequencies.

Using the previously optimized molecular geometries, i.e., for the isolated porphyrin and for the supramolecular arrangements, we calculated the electronic absorption spectra by vertical excitation within the TD-DFT framework performing single point calculations. A total of 50 excited states were calculated for each arrangement. Then, for one density functional used, we calculated a total of 950 excited states corresponding to 12 arrangements, three free monocationic porphyrins and four nucleotide pairs according to the position of the phosphate group. In the search to find the best functional that gives a reasonable description of the excited states, we used five density functionals (B3LYP [29–31], PBE0 [36, 37], CAM-B3LYP [38], M06-2X [39] and B97D [40]) and applied these to the **1A** and **1T** arrangements that contain porphyrin **1**. This means that 400 additional excited states were added, giving a total of 1,350 excited states in our study. The functional giving the least error for the Soret band in comparison with experimental values was then applied to the other arrangements. All excited state calculations were carried out with the basis set 6-31G(d). The hybrid functionals B3LYP and PBE0 have 20 % and 25 % of Hartree Fock exchange energy, respectively. The CAM-B3LYP functional contains non-local exchange from 19 % in the short-range limit to 65 % in the long-range limit and M06-2X contains 54 % non-local exchange at all ranges. The B97D functional replaces part of the nonlocal, long- and medium-range electron correlation effects and includes R^{-6} dependent terms [40]. B97D is a functional proved for thermochemical benchmarks, including transition metal chemistry, but this does not necessarily guarantee that it works well for excited states. The solvent water was also included in the calculation of the electronic spectra by means of the conductor-like polarizable continuum

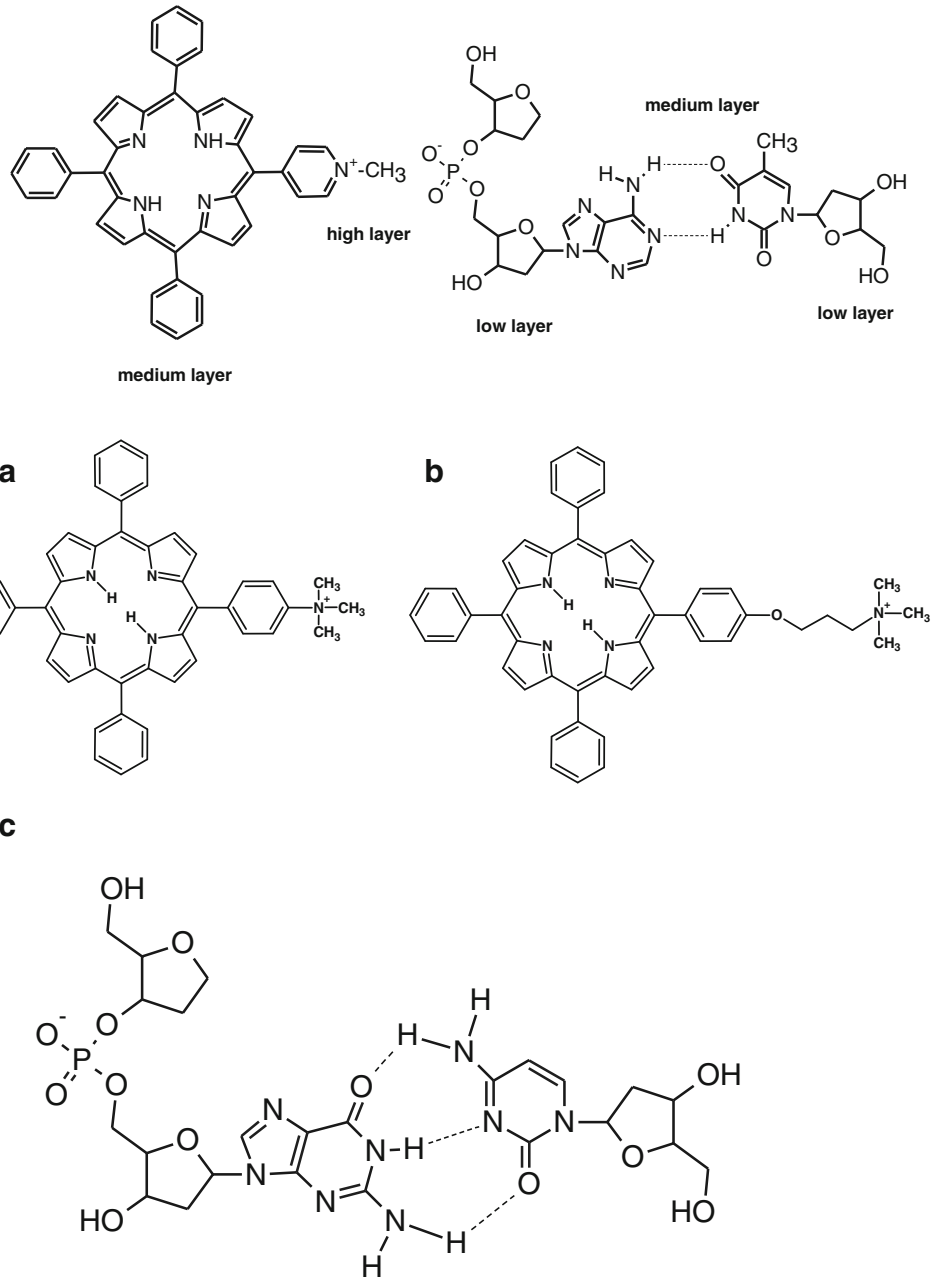

Fig. 1a c Structural model used to investigate the interaction between monocationic porphyrin meso-mono(N-methylpyridyl) triphenylporphyrin (**1**, $MmPyP^{+}$) and a nucleotide pair. As an example, we depict the adenine-thymine nucleotide pair (see text for details). **a 2,** MmAP+: Meso-mono (trimethylaniliniumyl) triphenylporphyrin; **b 3,** MONPP+: Meso-mono[(3-trimethylaminopropyl)oxiphenyl] triphenylporphyrin; **c** interaction of guanine-cytosine nucleotide pair

model (C-PCM) [41–44] and the Simple United Atom Topological Model for atomic radii.

Results and discussion

Estimation of the best functional for the electronic spectra

Based on our experience [45–48], electronic spectra are highly dependent on the density functional used, and hence we first performed a study to find the best functional able to give a reasonable prediction of the electronic spectra of the studied compounds.

We used two classical hybrid functionals, B3LYP and PBE0, one meta-hybrid GGA M06-2X, one long-range functional CAM-B3LYP, and Grimme's B97D functional including dispersion [40]. The latter three were chosen taking into account that cationic porphyrin approaches a nucleotide pair in non-covalent form (see Fig. 1). We tested the five functionals in the arrangements containing porphyrin **1** and adenine and thymine nucleotides, i.e., **1A** and **1T**, respectively (see Fig. 2), and analyzed the electronic spectra, particularly the Soret band that corresponds to the largest intensity band of the porphyrin. Table 1 shows the resulting excitation energies, wavelengths (λ) and oscillator strengths (*f*) for the Soret band calculated with the five functionals.

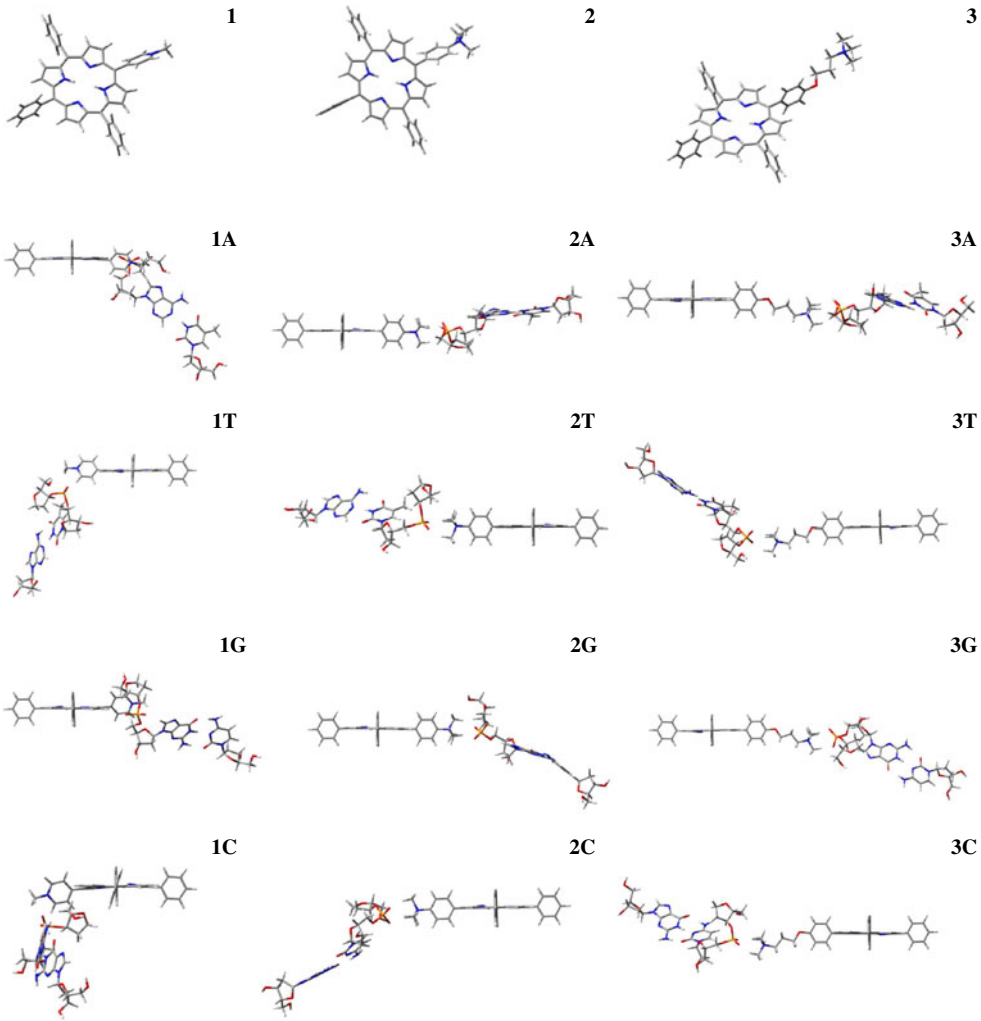

Fig. 2 Optimized molecular structures of the porphyrin-nucleotide pair arrangements (see text for details)

The theoretical results were compared with the available experimental data, which corresponds to the Soret band obtained for complexes formed between adenine-thymine polynucleotides (poly[d(A-T)]) and 5,10,15,20-tetrakis(4-methyl-pyridyl)porphyrin (TMPyP).

We found that CAM-B3LYP and M06-2X present similar behavior, the Soret band is blue-shifted with respect to the experimental data (437 nm) with a large deviation of ~12–13 % (~ −0.4 eV). The results show that these functionals seem to fail in the description of the Soret band. We note that both funtionals have higher values of exact exchange, suggesting that this could be responsible for the higher deviation with respect to experimental values. Although B97D predicts a red shift Soret band, its deviation with respect to experimental values is high (~19–21 %, 0.5 eV), indicating that the dispersion correction used is not the best for obtaining good prediction of the Soret band.

On the other hand, B3LYP and PBE0 yield a good description of the band, with the exception of **1T** with B3LYP, with a relative error of 2–3.9 % that represents no more than 0.1 eV. These errors are lower than other values reported for porphyrin derivatives [49, 50].

Considering that a monocationic instead of a tetracationic porphyrin was taken into account in the theoretical calculations, the excellent agreement between the B3LYP and PBE0 results and the experimental data, which includes the tetracationic porphyrin, suggests that only one cationic substituent is relevant in the interaction porphyrin–nucleotide pair. This would be true in the case of an outside binding, where the positive charge of the pyridyl substituent approachs the negative region of the phosphate group. Experimental values of Q bands for different ratio porphyrin–DNA associations are not available due to the smaller intensities in comparison with Soret. However, it is clear that the wavelengths of the Q bands of the porphyrins are also modified by interaction with DNA [15].

In order to decide which of the functionals (B3LYP or PBE0) to use, we investigated the electronic spectra of the tetracationic porphyrin **1′** and compared the results with the available experimental data (Table 2). As has been observed

Table 1 Excitation energy and oscillator force (*f*) corresponding to the Soret band for the supramolecular arrangements of **1** with the adenine (A)···thymine (T) nucleotide pair calculated in solution phase (water) for several density functionals using the basis set 6-31G(d)

	1A		**1T**		Exp.[a]
Functional	λ/nm (E/eV)	*f*	λ/nm (E/eV)	*f*	λ/nm (E/eV)
B3LYP	446 (2.78) (2.0%, 0.06)[d]	0.677	391 (3.17) (10%, −0.33)	0.566	430 (2.88) [b] 437 (2.84)[c]
PBE0	421 (2.94) (3.7%, −0.11)	1.087	420 (2.95) (3.9%, −0.11)	0.899	
M062X	386 (3.21) (11.7%, −0.37)	1.696	382 (3.24) (13.0%, −0.4)	1.632	
CAM-B3LYP	384 (3.23) (12.0%, −0.39)	1.728	380 (3.26) (13.0%, 0.42)	1.662	
B97D	520 (2.38) (−19%, 0.46)	0.163	530 (2.34) (−21%, 0.5)	0.092	

[a] UV-vis experimental values measured for complexes formed between adenine-thymine polynucleotide (poly[d(A-T)]) and 5,10,15,20-tetrakis (4-methyl-pyridyl)porphyrin (TMPyP) in solution at pH 6.9

[b] Ref. [17]

[c] Ref. [15]

[d] Relative error considering the more intense band with respect to the experimental value 437 nm (AT) and energy difference associated in eV

in previous works [45, 46, 48], the calculations predict two Q bands. The B3LYP absorptions at 589 and 559 nm agree well with the experimental values of 585 and 555 nm, respectively, with a deviation of 0.7 % (0.01 eV) in comparison with PBE0 (1 %). In B3LYP, these are slightly red-shifted, and in PBE0 they are blue-shifted.

For the Soret band, B3LYP calculations predict four absorptions with large oscillator strength (0.73–0.99) where the more intense band (364 nm) is blue-shifted with respect to experimental value (424 nm) with an error of 15 %. PBE0 calculations predict two important absorptions (450 and 442 nm) for the Soret band, where the more intense one (red-shifted) at 450 nm (f=0.881) shows a deviation of 6 % with respect to the experimental value of 424 nm. In accordance to the minor error introduced for the Soret band, we chose the functional PBE0 for analyzing porphyrin-DNA nucleotide pair arrangements. It is important to note that the functional PBE0 [36] has also been used with success by other authors in studies of electronic absorption [51, 52]. Considering that functionals are sensitive to the size of the molecules, some TD-DFT benchmarks have been carried out for the calculation of singlet-excited states of organic molecules [53]. In these studies, the functional PBE0 is proposed as the one giving the best match with reference data, which is attributed to the amount of the exact exchange in the range of 22–25 %.

Assessment of photosensitization properties of the arrangements

The theoretical results corresponding to the excitation energy, wavelength (λ), oscillator strength (*f*), electronic transition and its assignment for the arrangements having an outside binding by adenine side (**1A**), thymine side (**1T**), cytosine side (**1C**) and guanine side (**1G**) (Fig. 2) are shown in Table 3. In order to identify the effect that the nucleotide produces in the photosensitization of **1**, we present the more relevant absorption bands of **1** in Table 2. A comparative picture of the simulated spectra is shown in the Supplementary Material (Figure S1).

On the one hand, the experimental data (Tables 2, 3) show that the Soret band (424 nm) of the tetracationic porphyrin (**1′**) is shifted to a larger wavelength (red-shifted) (up to 20 nm) when porphyrin interacts with adenine-thymine polynucleotides (437 nm) or with guanine-cytosine polynucleotides (445 nm). This suggests that the capability of the tetracationic porphyrin as a photosensitizer, given the absorption seen in the visible region, is improved in the presence of nucleotides; the Soret band is red-shifted and therefore of lower energy.

From the point of view of theoretical calculations, Table 3 shows that all arrangements retain the characteristic absorption bands of porphyrins, i.e., a low intensity Q band and a high intensity Soret band. However, the position (λ) and intensity given by the oscillator strength (*f*) are modified due to the presence of the nucleotide pair, as happens for **1′** at the experimental level.

Overall, we found that, for all the arrangements shown in Table 3, the Q bands are blue-shifted with respect to **1** (581, 555 nm) in ~50 nm increments, and the intensities decreased. However, porphyrin **1** in the arrangement retains absorption ability in the visible region. The electronic transitions assigned to the Q bands (H→L and H-1→L or H→L + 1) show a small amount of charge transfer from

Table 2 Excitation energy for the more relevant excited states, oscillator force (*f*) and electronic transition assignments for tetracationic (**1′**) and monocation (**1**) porphyrins calculated at the B3LYP/6-31G(d) and PBE0/6-31G(d) levels of theory in solution phase (water). *CT* Charge transfer

1′				1				Exp.[a]
Assignment	λ/nm (E/eV)	*f*	Electronic Transition	Assignment	λ/nm (E/eV)	*f*	Electronic Transition	λ/nm (E/eV)
Q	589 (2.11)	0.013	H → L + 1	Q	602 (2.06)	0.241	H → L	585[d] (2.12)
	(0.7%, 0.01)[e]				(3%, 0.06)			650 (1.91)[b]
	579 (2.14)[d] (1%, −0.02)[d]	0.008[d]	H → L + 1[d]		581 (2.13)[d] (0.7%, 0.01) CT[d, e]	0.212[d]	H → L[d]	
	559 (2.22)	0.067	H → L		574 (2.16)	0.054	H-1 → L	520 (2.38)
	(0.7%, 0.01)[e]				(3.4%, 0.07)			555[d] (2.23)
	549 (2.26)[d] (1%, −0.03)[d]	0.063[d]	H → L[d]		555 (2.23)[d] (0%, 0.0) CT	0.072[d]	H-1 → L[d]	
Soret	462 (2.69)	0.811	H-1 → L	Soret	465 (2.67)	0.370	H → L + 1	424[d] (2.92)
	450 (2.76)[d]	0.881[d]	H-1 → L[d]		442 (2.80)[d]	0.516[d]	H → L + 1[d]	
	(6%, 0.16) CT[d, e]				457 (2.71)	0.257	H → L + 2	
	455 (2.72)	0.725	H-1 → L + 1		437 (2.83) CT[d]	0.433[d]	H → L + 2[d]	
	442 (2.80) CT[d]	0.836[d]	H-1 → L + 1[d]		382 (3.24)	0.634	H-1 → L + 2	
	364 (3.41)	0.998	H-3 → L		367 (3.37) CT[d]	0.691[d]	H-1 → L + 2[d]	
	(15%, −0.49)[c]				376 (3.30)	1.030	H-3 → L	
	435 (2.85) CT[d]	0.012[d]	H → L + **2**[d]		(11%, −0.38)[e]			
	360 (3.44)	0.998	H-3 → L + 1		361 (3.43)[d,e]	0.798[d]	H-4 → L[d]	
	423 (2.93) CT[d]	0.003[d]	H-1 → L + 2[d]		(15%, −0.51) CT[d,e]			

[a] UV-vis experimental values measured for 5,10,15,20-tetrakis(4-methyl-pyridyl)porphyrin (TMPyP) (**1′**) at pH 6.8

[b] Ref. [14]

[c] Relative error considering the more intense theoretical band[e] with respect to the experimental value 424 nm in % and energy difference associated in eV.

[d] PBE0/6-31G(d) level of theory

porphyrin to the pyridyl ring (Fig. 3), which is also present in free porphyrin **1**. Thus, the Q band assignments of **1** are not modified by interaction with the nucleotide pairs.

The Soret band for **1** is predicted at low wavelength (361 nm), and interaction with any nucleotide leads to a red-shift up to 60 nm, where the absorption energy is very similar for **1A** (421 nm), **1T** (420 nm) and **1G** (413 nm), but somewhat different for **1C** (371 nm). These results are in good agreement with the trend observed at the experimental level [15, 17]. This means that the effect of the nucleotide on the Soret band shifts the band to a longer wavelength.

It is important to mention that the arrangements used in the present study correspond to the minimum energy structures obtained in a previous work [24]. It was shown that **1** presents an affinity for each nucleotide in an outside binding mode with interaction energies in the range of~−60 to −80 kcal/mol^{-1} [24]. Thus, the present results would indicate that the favorable interaction between cationic porphyrin and nucleotide improves the capability of the porphyrin as a photosensitizer in the visible region. The similarity found for the more intense Soret band between **1A**, **1T** and **1G** leads to the conclusion that the cationic porphyrin **1** does not exhibit high selectivity toward nucleotides. This could be interpreted as a favorable characteristic because cationic porphyrin could be used widely as a photosensitizer with different polynucleotides (adenine-thymine or guanine-cytosine) without restriction.

Table 3 shows the five more relevant absorptions of the Soret band and includes the electronic transitions between the molecular orbitals in order to understand the nature of such absorptions.

For all the arrangements, we found that the Soret band corresponds to electronic transitions between the occupied molecular orbitals (MO) homo (highest occupied) (H), homo-1 (H-1) and homo-5 (H-5) and the unoccupied molecular orbitals lumo (lowest unoccupied) (L), lumo + 1 (L + 1) and lumo + 2 (L + 2). Figure 3 shows the surfaces of the molecular orbitals obtained in solution (water) at the PBE0/6-31G(d) level of theory that are important in the analysis of Soret and Q bands. A large number of these transitions present a charge transfer from the porphyrin core to the pyridyl ring belonging to the porphyrin. A similar behavior was found for the Soret band of **1** and **1′**, i.e., a charge transfer porphyrin → pyridyl. This means that the

Table 3 Excitation energy for the more relevant excited states, oscillator force (*f*), and electronic transitions assignment for the supramolecular arrangements of **1** with adenine (A)···thymine (T) and guanine (G)···cytosine (C) nucleotide pairs at the PBE0/6-31G(d) level of theory in solution phase (solvent water)

1A				1T				Exp.[a]
Assignment	λ/nm (E/eV)	*f*	Electronic Transition	Assignment	λ/nm (E/eV)	*f*	Electronic Transition	λ/nm (E/eV)
Q	537 (2.31)	0.066	H → L	Q	535 (2.32)	0.033	H → L	
	518 (2.39)	0.032	H-1 → L		516 (2.40)	0.018	H-1 → L	
Soret	421 (2.95)[f]	1.087	H-1 → L + 1	Soret	420 (2.95)[f]	0.899	H → L + 2 CT	430 (2.88) [b],
	(3.7%, −0.11)[d, f]	0.730	H-1 → L CT		(3.9%, −0.11)[d, f]	0.739	H-1 → L CT	437 (2.84)[c]
	412 (3.01)	0.387	H → L + 2 CT		409 (3.03)	0.519	H → L + 2 CT	
	379 (3.27)	0.185	H-1 → L + 2 CT		383 (3.24)	0.203	H-1 → L + 2 CT	
	366 (3.39)	0.331	H-5 → L CT		368 (3.37)	0.321	H-5 → L CT	
	362 (3.43)				362 (3.42)			
1G				1C				Exp.[e]
Q	545 (2.27)	0.062	H → L	Q	545 (2.27)	0.042	H → L	
	520 (2.38)	0.020	H-1 → L		521 (2.38)	0.023	H → L + 1	
Soret	415 (2.99)	0.781	H-1 → L CT	Soret	425 (2.92)[f]	0.523	H → L + 2 CT	444 (2.79)[b]
	413 (3.00)[d]	0.962	H-1 → L + 1		421 (2.94)[f]	0.511	H-1 → L CT	445 (2.79)[c]
	(7%, −0.21)[f]							
	373 (3.32)	0.030	H → L + 2 CT		390 (3.18)	0.389	H → L + 2 CT	
	371 (3.34)	0.118	H-1 → L + 2 CT		383 (3.24)	0.514	H-1 → L + 2 CT	
	364 (3.41)	0.732	H → L + 2 CT		371 (3.34)[d,f]	0.661	H-5 → L CT	
					(17%, −0.55)[f]			

[a] UV-vis experimental values measured for complexes formed between adenine-thymine polynucleotides (poly[d(A-T)]) and 5,10,15,20-tetrakis (4-methyl-pyridyl)porphyrin (TMPyP)

[b] Ref. [17]

[c] Ref. [15]

[d] Relative error considering the more intense band with respect to the experimental value 437 nm (AT) and 445 nm (GC) in % and energy difference in eV

[e] UV-vis experimental values measured for complexes formed between guanine-cytosine polynucleotides (poly[d(G-C)]) and 5,10,15,20-tetrakis (4-methyl-pyridyl)porphyrin (TMPyP)

[f] The more intense Soret band

nature of the Soret band is conserved, so the interaction of **1** with nucleotides is seen as favorable.

On the other hand, we investigated how the absorption of nucleotide pairs is affected by the presence of porphyrin **1**. According to the results, for PBE0/6-31G(d) in solution phase (water), the longer wavelength to which the isolated nucleotide pairs of the arrangements absorb occurs in the UV region, with values of 257 nm (1A), 261 nm (1T), 291 nm (1G) and 293 nm (1C). We found that when **1** interacts with nucleotide pairs, a red-shift of the absorption is produced with a decrease in oscillator strength, i.e., 284 nm (1A), 280 nm (1T), 297 nm (1G) and 294 nm (1C). As can be seen, the effect of **1** on the adenine-thymine nucleotide pair is larger than that on the guanine-cytosine nucleotide pair. A possible explanation could be related to the different π electronic structure of the nucleotides that is responsible for the excitation.

Up to this point, we have discussed results for **1** and the arrangements of the position (wavelength) of the Soret band and the electronic transitions associated with this molecule, as well as the nature of the transitions in terms of MOs. But what explains the red-shifting of Soret band that the arrangements show?

Figure 4 illustrates the MO energies (six occupied and six unoccupied) for **1** and the arrangements that allow the effect of the nucleotides to be understood. Arrows indicate the electronic transition corresponding to the more intense Soret band, and the MO surfaces involved in that transition are also depicted. The effect of the nucleotides on **1** can be seen as a destabilization (increased energy) of the occupied MOs (with exception of HOMO), LUMO and some unoccupied MOs. A near degeneration between occupied MOs as well as between unoccupied MOs is also found as a result of the interaction of **1** with the nucleotide pair. It is interesting to note that the HOMO–LUMO gap of the arrangements corresponding to the ground state calculated with PBE0/6-31G(d) in the solution phase (water) increases with respect to **1** (2.63eV), with values of

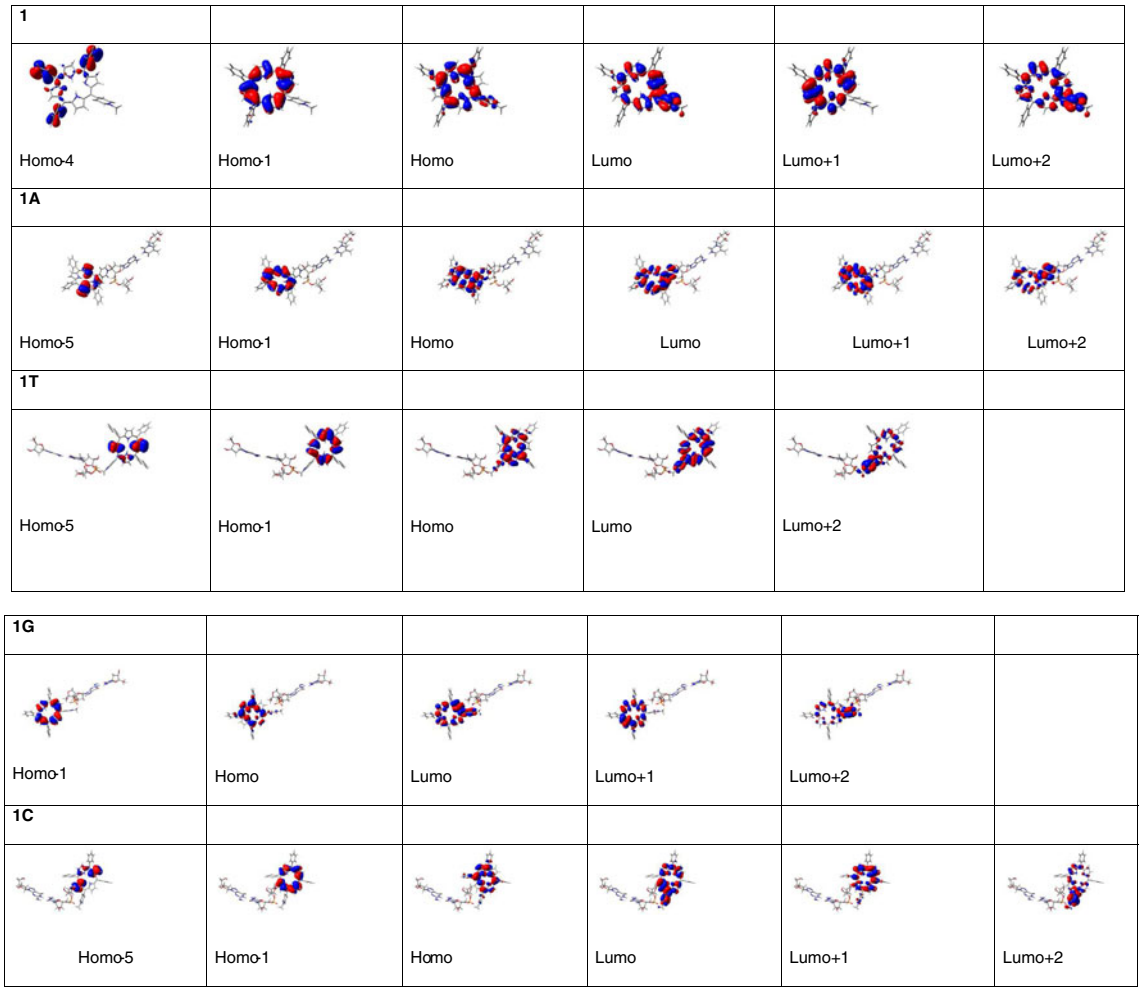

Fig. 3 Surfaces of the more relevant molecular orbitals of the arrangements **1A**, **1T**, **1G**, **1C** and free porphyrin **1** obtained at the PBE0/6-31G(d) level of theory in solution phase (water)

3.02, 3.07, 2.95 and 2.96 for **1A**, **1T**, **1G** and **1C**, respectively. The higher stabilization of the arrangements denoted by a larger HOMO–LUMO gap could be explained in terms of the higher symmetry found for these arrangements. The latter is verified by the dipole moment values shown in Table 4. Note that the correlation between HOMO–LUMO gap and the dipole moment does not correspond necessarily to a directly proportional relationship. Other factors besides symmetry could determine a larger HOMO–LUMO gap. A larger symmetry in a molecular structure implies a lower dipole moment. Porphyrin **1,** as shown in Table 4, presents a dipole moment value of 27.7D, which is larger than in the arrangements, 15.5D (1A), 21.3D (1T), 8.7D (1G) and 18.8D (1C).

On the other hand, a higher symmetry in a molecular structure implies a more symmetrical distribution of the electronic density, which affects directly the formation of an excited state. In relation to **1**, the higher symmetry presented by all the arrangements could explain the larger wavelength (shorter energy) found for the absorption of the Soret band (Table 3). It is clear that the intermolecular interaction between **1** and the nucleotide pairs generates electrostatic interaction and hydrogen bonding that also affects the distribution of electronic density. The asymmetric distribution of electronic density of HOMO-4 in **1** (Fig. 3), which is located along the three phenyl rings in the meso position, leads to a larger excitation energy for the Soret band (HOMO-4 → LUMO) than in the arrangements. In **1A**, **1T** and **1G**, the surface of the occupied MO involved in the Soret band is very similar to that of the unoccupied MO of the same band, and a small amount of charge transfer is obtained from the porphyrin core to the pyridyl ring. In the case of **1C**, where the electronic transition corresponds to HOMO-5 → LUMO, a larger charge transfer that goes from one pyrrole ring to the other, and also toward the pyridyl ring, can be observed (Fig. 4), implying a larger excitation energy. Thus, the red shift of the electronic absorption obtained for the arrangements with porphyrin **1** could be explained by taking into account the dipole moment and the symmetry of the MOs.

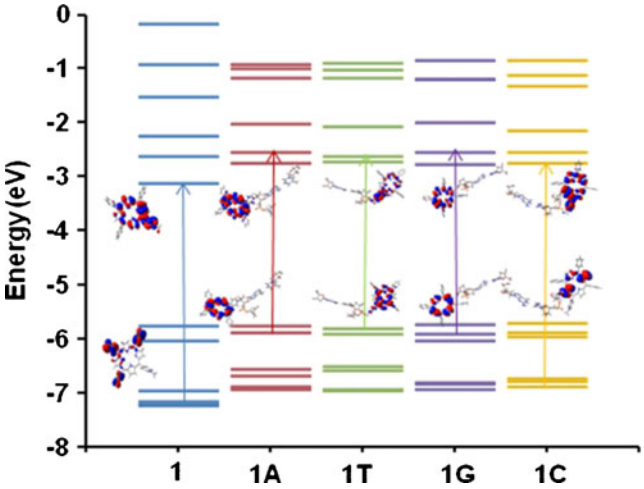

Fig. 4 Molecular orbital (MO) depiction of the more relevant occupied and unoccupied energy levels for the free monocationic porphyrin (**1**) and the arrangements (1A, 1T, 1G, 1C) calculated at the PBE0/6-31G(d) level of theory. Surfaces involved in the more intense Soret band are also included (see text for details). *Arrows* indicate the most important electronic transition of the Soret band between an occupied and an unoccupied MO

We also investigated other types of cationic porphyrin, **2** [54, 55] and **3** [56, 57] (Fig. 1), which differ with respect to **1** in the size of the substituent and in the position of the positive charge. In both porphyrins, the positive charge belongs to a tri-methyl amino group, in contrast to **1** where this charge resides in a pyridyl ring. The same molecular model was used, i.e., a porphyrin approaching the nucleotide pairs by outside binding. These kind of compounds have been synthesized and probed as bounding molecules to DNA [54, 57].

Tables 5 and 6 show the wavelength (excitation energy), oscillator strength and electronic transition for the Soret and Q bands calculated for the arrangements of **2** and **3**, respectively, at the PBE0/6-31G(d) level of theory in the solution phase (solvent water). Experimental values are also included. Initially, we found that all the theoretical bands are calculated at lower wavelengths than experimental ones. The deviation of the Soret band is in the range of 4–8%, with the arrangements presenting a higher deviation. Taking as a reference the isolated cationic porphyrin (**2**, **3**), we found that the Soret and Q bands of the arrangements are blue shifted. The intensity and the nature of the bands are kept for the latter. In particular, we observed in **2** (394 nm), a blue shift of 4 nm (390 nm) for the Soret band for all the arrangements (**2A**, **2T**, **2G**, **2C**). In the case of **3**, no change in the Soret band was observed for the arrangements; the more intense band corresponds to 390 nm. In the context of the structural model used, i.e., porphyrin-nucleotide pairs, these results suggest that, for an outside binding, the larger monocationic substituents do not improve the photosensitization properties. This can be understood in terms of a weak interaction between the nucleotides and the porphyrin core.

Although at the experimental level the interaction of **2**-DNA and **3**-DNA produces a red shift of the Soret band, the shift corresponds to 4–8 nm, which is lower than in **1** (13–21 nm). Thus, our theoretical results also indicate that the structural model constituted by porphyrin-nucleotide pairs interacting by outside binding is limited and not enough to predict experimental trends. A way to improve the model could be the inclusion of a sequence of nucleotides approaching a more accurate picture and closer to actual DNA.

Table 4 Dipole moment (μ) values (debye) for free porphyrin and the arrangements calculated at the PBE0/6-31G(d) level of theory in solution phase (solvent water)

	μ		μ		μ
1	27.7	**2**	36.9	**3**	54.7
1A	15.5	**2A**	16.2	**3A**	12.9
1T	21.3	**2T**	17.3	**3T**	15.9
1G	8.7	**2G**	11.9	**3G**	6.9
1C	18.8	**2C**	23.8	**3C**	25.8

Conclusions

We have presented a theoretical study at the DFT level of theory and using TD-DFT methodology on the photosensitization properties of three monocationic porphyrins (**1**–**3**) that differ in the size of the cationic substituent and that interact by outside binding with DNA nucleotide pairs [adenine (A)-thymine (T); guanine (G)-cytosine (C)]. An initial study to test the best density functional was performed for the cationic porphyrin with the smaller substituent (**1**). Thus, B3LYP, PBE0, CAM-B3LYP, M06-2X and B97D with the 6-31G(d) basis set at the solution phase (water) were used. The best agreement with experimental data of the electronic spectra was found for the functional PBE0. We analyzed the characteristics of the porphyrin, Soret and Q bands, and found that the effect of nucleotides on **1** is a red-shift of the Soret band (up to 60 nm), in agreement with experimental data, and a blue-shift of the Q band in agreement with the increasing stability of the arrangements. The larger symmetry for the arrangements of **1**, in comparison with free porphyrin, given by a lower dipole moment and a more symmetric distribution of the electronic density found by the MOs, could explain the lower excitation energy and the red shift of the Soret band.

The results indicate that porphyrin **1** improves its characteristics as photosensitizer when it interacts with DNA nucleotide pairs because the absorption requires longer wavelengths (red-shift band). Larger substituents in monocationic porphyrins do not present the same behavior, in contrast with experimental trends. We conclude that the structural model is insufficient for larger substituents and

Table 5 Excitation energy for the more relevant excited states, oscillator force (*f*), and electronic transitions assignment for **2** and the supramolecular arrangements with adenine (A)···thymine (T) and guanine (G)···cytosine (C) nucleotide pairs at the PBE0/6-31G(d) level of theory in solution phase (solvent water)

		2						Exp.[a]
		Assignment	λ/nm (E/eV)	*f*	Electronic transition			
		Q	540 (2.29)	0.037	H → L			
			515 (2.41)	0.011	H → L + 1			
		Soret	403 (3.08)	1.086	H-1 → L + 1			414 (2.99)[b]
			394 (3.15)[f] (4.6%, −0.15)[f]	1.493	H-1 → L			413 (3.00)[c]
2A				2T				Exp.[a]
Assignment	λ/nm (E/eV)	*f*	Electronic Transition	Assignment	λ/nm (E/eV)	*f*	Electronic Transition	λ/nm (E/eV)
Q	533 (2.33)	0.025	H → L	Q	534 (2.32)	0.028	H → L	
	509 (2.44)	0.001	H → L + 1		509 (2.43)	0.003	H → L + 1	
Soret	399 (3.11)	1.052	H-1 → L + 1	Soret	398 (3.12)	1.089	H-1 → L + 1	424 (2.92)[d]
	390 (3.18)[e,f]	1.432	H-1 → L		390 (3.18)[e, f]	1.400	H-1 → L	425 (2.92)[b]
	(7%, −0.24)[f]				(7%, −0.24)[f]			421 (2.94)[c1]
2C				2G				Exp.[a]
Q	533 (2.33)	0.025	H → L	Q	534 (2.32)	0.028	H → L	
	509 (2.44)	0.001	H → L + 1		509 (2.43)	0.003	H → L + 1	
Soret	399 (3.11)	1.059	H-1 → L + 1	Soret	398 (3.12)	1.088	H-1 → L + 1	425 (2.92)[b]
	390 (3.18)[e,f] (6.6%, −0.21)[f]	1.405	H-1 → L		390 (3.18)[e, f] (6.6%, −0.21)[f]	1.401	H-1 → L	418 (2.97)[c2]

[a] UV-vis experimental values measured for tetracationic porphyrins

[b] Ref. [13]

[c] Ref. [54], [c1] sequential oligonucleotide $(dA\text{-}dT)_{10}$ [c2] sequential oligonucleotide $(dG\text{-}dC)_{10}$

[d] Ref. [55]

[e] Relative error considering the more intense band with respect to the experimental value 421 nm (AT) and 418 nm (GC) in % and energy difference in eV

[f] The more intense Soret band

Table 6 Excitation energy for the more relevant excited states, oscillator force (*f*), and electronic transitions assignment for **3** and the supramolecular arrangements with adenine (A)···thymine (T) and guanine (G)···cytosine (C) nucleotide pairs at the PBE0/6-31G(d) level of theory in solution phase (solvent water)

		3						
		Assignment	λ/nm (E/eV)	*f*	Electronic transition			Exp.[a]
		Q	533 (2.32)	0.026	H → L			583 (2.13)[b]
								640 (1.94)
			509 (2.44)	0.002	H → L + 1			520 (2.38)
								558 (2.22)
		Soret	398 (3.12)	1.074	H-1 → L + 1			418 (2.97)
			390 (3.18)[f]	1.421	H-1 → L			
			(6.7%, −0.21)[f]					
3A				3T				Exp.[a]
Assignment	λ/nm (E/eV)	*f*	Electronic Transition	Assignment	λ/nm (E/eV)	*f*	Electronic transition	λ/nm (E/eV) Soret
Q	533 (2.33)	0.028	H → L	Q	533 (2.33)	0.027	H → L	
	509 (2.44)	0.002	H → L + 1		509 (2.44)	0.001	H → L + 1	
Soret	398 (3.12)	1.081	H-1 → L + 1	Soret	398 (3.12)	1.077	H-1 → L + 1	424 (2.92)[b]
	390 (3.18)[d]	1.411	H-1 → L		390 (3.18)[d, f]	1.401	H-1 → L	425 (2.92)[c1]
	(8%, −0.26)[f]				(8%, −0.26)[f]			
3C				3G				Exp.[a]
Q	533 (2.36)	0.027	H → L	Q	533 (2.33)	0.027	H → L	
	509 (2.44)	0.002	H → L + 1		509 (2.44)	0.001	H → L + 1	
Soret	398 (3.12)	1.076	H-1 → L + 1	Soret	398 (3.12)	1.078	H-1 → L + 1	424 (2.92)[b]
	390 (3.18)[d, f]	1.419	H-1 → L		390 (3.18)[d,f]	1.380	H-1 → L	422 (2.94)[c2]
	(7.6%, −0.24)[f]				(7.6%, −0.24)[f]			

[a] UV-vis experimental values measured for tetracationic porphyrins

[b,c] Ref. [56], [c1] $[poly(dA\text{-}dT)]_2$, [c2] $[poly(dG\text{-}dC)]_2$

[d] Relative error considering the more intense band with respect to the experimental value 425 nm (AT) and 422 nm (GC) in % and energy difference in eV

[f] The more intense Soret band

that photosensitization to longer wavelengths is favored for porphyrins with a cationic charge in the pyridyl ring and a small substituent, which improves communication between the porphyrin core and the nucleotide pair. Use of a sequence of nucleotides is suggested to obtain a more accurate picture of the photosensitization of porphyrin with larger substituents.

Acknowledgments G.I.C.J. thanks the financial support of Comisión Nacional de Investigación Científica y Tecnológica de Chile (CONICYT)-CHILE from Project FONDECYT N°1090700 and Departamento de Investigaciones Científicas y Tecnológicas (DICYT)–The University of Santiago of Chile (USACH) from Project Complementary Support by computational time. L.C. thanks to CONICYT by Doctoral Fellowship.

References

1. Burger RM (1998) Chem Rev 98:1153–1170
2. Tjahjono DH, Akutsu T, Yoshioka N, Inoue H (1999) Biochim Biophys Acta 1472:333–343
3. Munson BR, Fiel RJ (1992) Nucleic Acids Res 20:1315–1319
4. Garcia G, Sarrazy V, Sol V, Morvan CL, Granet R, Alves S, Krausz P (2009) Bioorg Med Chem 17:767–776
5. Martino L, Pagano B, Fotticchia I, Neidle S, Giancola C (2009) J Phys Chem B 113:14779–14786
6. Shi D-F, Wheelhouse RT, Sun D, Hurley LH (2001) J Med Chem 44:4509–4523
7. Mező G, Herényi L, Habdas J, Majer Z, Myśliwa-Kurdziel B, Tóth K, Csík G (2011) Biophys Chem 155:36–44
8. Nyman ES, Hynninen PH (2004) J Photochem Photobiol B Biol 73:1–28
9. Kasturi C, Platz MS (1992) Photochem Photobiol 56:427–429
10. Wainwright M (2003) Int J Antimicrob Agents 21:510–520
11. Zupán K, Herényi L, Tóth K, Majer Z, Csík G (2004) Biochemistry 43:9151–9159
12. Dixon DW, Schinazi R, Marzilli LG (1990) Ann N Y Acad Sci 616:511–513
13. Carvlin MJ, Fiel RJ (1983) Nucleic Acids Res 11:6121–6139
14. Fiel RJ, Howard JC, Mark EH, Gupta ND (1979) Nucleic Acids Res 6:3093–3118
15. Kelly JM, Murphy MJ, McConnell DJ, OhUigin C (1985) Nucleic Acids Res 13:167–184
16. McMillin DR, Shelton AH, Bejune SA, Fanwick PE, Wall RK (2005) Coord Chem Rev 249:1451–1459
17. Pasternack RF, Gibbs EJ, Villafranca JJ (1983) Biochemistry 22:2406–2414
18. Marzilli LG, Petho G, Lin M, Kim MS, Dixon DW (1992) J Am Chem Soc 114:7575–7577
19. Villanueva A, Jori G (1993) Cancer Lett 73:59–64
20. Quiroga ED, Cormick MP, Pons P, Alvarez MG, Durantini EN (2012) Eur J Med Chem 58:332–339
21. Cano M, Castillero P, Roales J, Pedrosa JM, Brittle S, Richardson T, González-Elipe AR, Barranco A (2010) Sensors Actuators B Chem 150:764–769
22. Nitzan Y, Ashkenazi H (2001) Curr Microbiol 42:408–414
23. de Sousa Neto D, Tabak M (2012) J Colloid Interface Sci 381:73–82
24. Cárdenas-Jirón GI, Cortez-Santibañez L (2013) J Mol Model 19:811–824
25. Svensson M, Humbel S, Froese RDJ, Matsubara T, Sieber S, Morokuma K (1996) J Phys Chem 100:19357–19363
26. Humbel S, Sieber S, Morokuma K (1996) J Chem Phys 105:1959–1967
27. Dapprich S, Komáromi I, Byun KS, Morokuma K, Frisch MJ (1999) J Mol Struct (THEOCHEM) 461–462:1–21
28. Frisch MJ, Trucks GW, Schlegel HB, Scuseria GE, Robb MA, Cheeseman JR, Montgomery JA, Vreven JT, Kudin KN, Burant JC, Millam JM, Iyengar SS, Tomasi J, Barone V, Mennucci B, Cossi M, Scalmani G, Rega N, Petersson GA, Nakatsuji H, Hada M, Ehara M, Toyota K, Fukuda R, Hasegawa J, Ishida M, Nakajima T, Honda Y, Kitao O, Nakai H, Klene M, Li X, Knox JE, Hratchian HP, Cross JB, Bakken V, Adamo C, Jaramillo J, Gomperts R, Stratmann RE, Yazyev O, Austin AJ, Cammi R, Pomelli C, Ochterski JW, Ayala PY, Morokuma K, Voth GA, Salvador P, Dannenberg JJ, Zakrzewski VG, Dapprich S, Daniels AD, Strain MC, Farkas O, Malick DK, Rabuck AD, Raghavachari K, Foresman JB, Ortiz JV, Cui Q, Baboul AG, Clifford S, Cioslowski J, Stefanov BB, Liu G, Liashenko A, Piskorz P, Komaromi I, Martin RL, Fox DJ, Keith T, Al-Laham MA, Peng CY, Nanayakkara A, Challacombe M, Gill PMW, Johnson B, Chen W, Wong MW, Gonzalez C, Pople JA (2007) Gaussian, Wallingford CT
29. Becke AD (1988) Phys Rev A 38:3098–3100
30. Becke ADJ (1993) Chem Phys 98:5648–5652
31. Lee C, Yang W, Parr RG (1988) Phys Rev B 37:785–789
32. Stewart JJP (1989) J Comput Chem 10:209–220
33. Rappe AK, Casewit CJ, Colwell KS, Goddard WA, Skiff WM (1992) J Am Chem Soc 114:10024–10035
34. Sundaresan N, Pillai CKS, Suresh CH (2006) J Phys Chem A 110:8826–8831
35. Sundaresan N, Suresh CH (2007) J Chem Theory Comput 3:1172–1182
36. Adamo C, Barone V (1999) J Chem Phys 110:6158–6170
37. Ernzerhof M, Scuseria GEJ (1999) Chem Phys 110:5029–5036
38. Yanai T, Tew DP, Handy NC (2004) Chem Phys Lett 393:51–57
39. Zhao Y, Truhlar D (2008) Theor Chem Accounts Theory Comput Model (Theor Chim Acta) 120:215–241
40. Grimme S (2006) J Comput Chem 27:1787–1799
41. Cossi M, Barone VJ (2001) Chem Phys 115:4708–4717
42. Improta R, Barone V, Santoro F (2007) Angew Chem Int Ed 46:405–408
43. Santoro F, Barone V, Gustavsson T, Improta RJ (2006) Am Chem Soc 128:16312–16322
44. Scalmani G, Frisch MJ, Mennucci B, Tomasi J, Cammi R, Barone VJ (2005) Chem Phys 124:94107–94121
45. Cárdenas-Jirón GI, Barboza CA, López R, Menéndez MI (2011) J Phys Chem A 115:11988–11997
46. López R, Menéndez M, Santander-Nelli M, Cárdenas-Jirón G (2010) Theor Chem Accounts Theory Comput Model (Theor Chim Acta) 127:475–484
47. Yáñez M, Guerrero J, Aguirre P, Moya SA, Cárdenas-Jirón G (2009) J Organomet Chem 694:3781–3792
48. Palma M, Cárdenas-Jirón GI, Menéndez Rodríguez MI (2008) J Phys Chem A 112:13574–13583
49. Petit L, Quartarolo A, Adamo C, Russo N (2006) J Phys Chem B 110:2398–2404
50. Quartarolo AD, Russo N, Sicilia E, Lelj F (2007) J Chem Theory Comput 3:860–869
51. Alberto ME, De Simone BC, Cospito S, Imbardelli D, Veltri L, Chidichimo G, Russo N (2012) Chem Phys Lett 552:141–145
52. Adamo C, Barone V (1999) Chem Phys Lett 314:152–157
53. Jacquemin D, Wathelet VR, Perpète EA, Adamo C (2009) J Chem Theory Comput 5:2420–2435
54. Nový J, Urbanová M (2007) Biopolymers 85:349–358
55. Hong S, Huh S (2003) Bull Korean Chem Soc 24:137–140
56. Mukundan NE, Petho G, Dixon DW, Kim MS, Marzilli LG (1994) Inorg Chem 33:4676–4687
57. Mukundan NE, Petho G, Dixon DW, Marzilli LG (1995) Inorg Chem 34:3677–3687